STRESS-STRAIN BEHAVIOUR AND SOFTENING IN MANGANESE TWIP STEEL TESTED IN THERMAL-MECHANICAL SIMULATOR

PLASTOMETRICKÉ VÝSLEDKY NAPĚŤOVO-DEFORMAČNÍHO CHOVÁNÍ A STUPNĚ ZMĚKČENÍ FEROMANGANOVÉ TWIP OCELI

Jiří Kliber, Kamil Drozd, Ilja Mamuzić

VŠB - TU of Ostrava, Department of Materials Forming, 17. listopadu 15, 708 33, Ostrava, Czech Republic, jiri.kliber@vsb.cz, kamil.drozd@vsb.cz

Abstract

The ferromanganese TWIP steels with content of 17 to 20 % of manganese are fully austenitic and non-magnetic, without any phase transformation. Owing to the claiming of the twinning mechanism the TWIP-steels are able to satisfy a great number of technical requirements for production of cars of the new generation. The primary experimental results of the TWIP-steels show the high end tensile strength of 600 to 1100 MPa und extreme values of ductility at intervals from 60 % to 90 %. Through the method of plasma and vacuum melting there were prepared alloyed castings Fe-Mn-C. The samples with dimension of 8,5 x 15 x 20 mm were put to plasto-metrically checking (PSCT) on the Gleeble 3500. As variables there were selected temperatures from 900 ºC to 1100 ºC. The tests were both continuous with the deformation e = 0,8 as discontinuous with the consecutive deformations e_1 up to e_3 = 0,3 and with the terms between the draughts from 1 second to 100 seconds. The major section of the experimental works was focused on the monitoring of the influence of the forming work on the structural and the mechanical characteristics of the highly solid TWIP-steels Fe-Mn in dependence on the different chemical structure of the particular samples. The objective of this contribution is the evaluation of the dependence tension/deformation, determination of the constants for the mathematically equations for tension/deformation and determination of the point of the softening of the structure X.

Abstrakt

Feromanganové TWIP oceli s obsahem 17 až 20 % manganu jsou plně austenitické a nemagnetické, bez fázové transformace. Vzhledem k uplatnění mechanismu dvojčatění jsou TWIP oceli schopny uspokojit řadu technických požadavků pro výrobu aut nové generace. Základní experimentální výsledky TWIP ocelí vykazují vysokou konečnou pevnost v tahu 600 až 1100 MPa a extrémní hodnoty tažnosti v rozmezí 60 % až 90 %. Metodou plazmového a vakuového tavení byly připraveny odlitky slitin Fe-Mn-C. Vzorky o rozměrech 8,5 x 15 x 20 mm byly podrobeny plastometrickému zkoušení (PSCT) na Gleeblu 3500. Jako proměnné byly zvoleny teploty od 900 ºC do 1100 ºC. Zkoušky byly jednak spojité s deformací e = 0,8, tak i přerušované s postupnými deformacemi e_1 až e_3 = 0,3 a s časy mezi úběry od 1 s do 100 s. Hlavní část experimentálních prací byla zaměřena na sledování vlivu tváření na strukturní charakteristiky a mechanické vlastnosti vysoce pevných Fe-Mn TWIP ocelí v závislosti na rozdílném chemickém složení jednotlivých vzorků. Cílem příspěvku je vyhodnotit závislost napětí-deformace, určit konstanty do matematických rovnic napětí-deformace a stanovit stupeň změkčení struktury X.

1. THEORETICAL FUNDAMENTALS OF TWIP STEELS

For quite some time, steel manufacturers have observed that they faced the competition of aluminium and other new materials, such as magnesium alloys or plastics. In order to remain competitive, the new steels have to be lighter, stronger and more stable. One of the materials which could fulfil such demand in future is TWIP steel.

The growing requirements for the car body design are equal in importance to the properties and quality of steels used. During a crash, the steel parts of the car body should meet two different requirements: they must be ductile (tough) to be able to absorb as much crash energy as possible, but also stable in shape to protect the passengers in the cabin. Materials, which could satisfy these requirements, include in the first place high-manganese TWIP steels with 17 – 20% Mn. These austenitic steels exhibit exceptional properties thanks to a special strengthening mechanism based on twinning [2].

Manganese TWIP steels with 17 to 20% Mn are fully austenitic and non-magnetic and undergo no phase transformation. Mechanical twins cause large strengthening during straining, prevent necking under tensile load and provide the material with high strength. Initial results of experiments with the TWIP steel brought the ultimate tensile strength between 600 and 100 MPa and an extreme elongation between 60% and 90%.

TWIP steels are popular mainly due to their large shock absorbing capacity. It is more than twice as large as in conventional high-strength steels. TWIP steels undergo deformation upon a mechanical shock but still retain their ductility. Every location of the steel part first elongates, strengthens and then transmits the rest of the strain energy to its neighbouring locations which deform as well. Owing to the distribution of energy across the whole surface, the shock energy absorbs much more efficiently, which gives the car passengers better chances of surviving the crash.

Twinning causes marked increase in the strain hardening coefficient value (n), as the microstructure of steel becomes ever finer. High-manganese TWIP steels combine extremely high strength and very good ductility as the newly-formed twin boundaries act as grain boundaries in terms of strengthening the material. The hardening coefficient n increases to 0,4 at strains of about 30% and then remains constant up to the total elongation of 50% [1].

The suitability of TWIP steels for existing manufacturing procedures used for other steel grades, including the subsequent continuous casting, rolling, pressing, and also their good weld ability should rank among their advantages. Minor technical difficulties might occur during metallurgical production of these steels. A portion of manganese might be lost during melting due to high manganese vapour pressure. Evaporation of significant portion of manganese during melting requires that it is added in greater amounts [2].

2. EXPERIMENTAL

Specimens with dimensions of 8,5x15x20 mm were tested in a Gleeble 3500 thermal-mechanical simulator. Initial testing parameters are listed in tables 1 and 2. Further experiments included continuous testing at temperatures ranging from 900 to 1100 °C. For some of the tests, strain rates of up to 100 s^{-1} were used [2].

Table 1. Parameters of plastometric testing of specimens p1 through p6

strain rate ė	strain e	temperature [°C]	cooling method	specimen
5	0,8	1100	air	p1
		1100	water	p2
		1000	air	p3
		1000	water	p4
		900	air	p5
		900	water	p6

Table 2. Parameters of plastometric testing of specimens p7 through p18

strain rate ė	strain e	delay time [s]	temperature [°C]	
			1100	900
1	0,3	1	p7	p13
		10	p8	p14
		100	p9	p15
10		1	p10	p16
		10	p11	p17
		100	p12	p18

Actual results of the continuous load experiments are shown in Fig. 1. Owing to large number of experimental values, only the actual strain-related results were used. Of these, every fifth value was chosen.

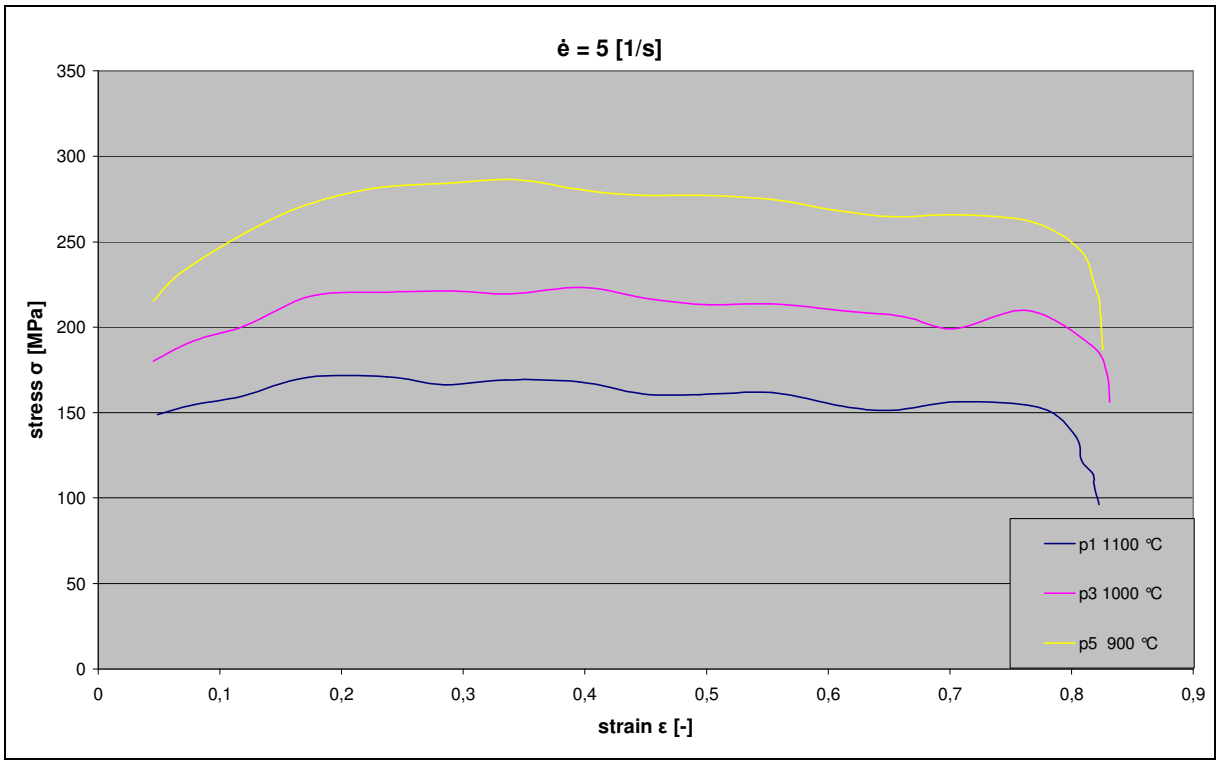

Fig. 1. Stress-strain relationship in specimens p1, p3 and p5

The technique of stepwise determination of σ_{pc} according to equation (1) was chosen for comprehensive examination and construction of stress-strain curves [3-9].

$$\sigma_{pc} = \frac{1}{\alpha} \operatorname{arcsin} h \left(\frac{\dot{\varepsilon} \cdot \exp \frac{Q}{RT}}{A} \right)^{\frac{1}{n}} \tag{1}$$

Successive linear regression calculations, calculation of constants n, α, β and application of the sinh equation yielded the activation energy value of Q = 581 KJ/mol. The following stage involved determination of ε_{pc} using the equation (2).

$$\varepsilon_{pc} = \dot{\varepsilon}^{k} \cdot \exp \operatorname{arcsin} h \left(Y + \frac{X}{T} \right) \tag{2}$$

Complete stress-strain curves were described by equations (3) [10].

$$\sigma_{c} = \sigma_{pc} \left[\frac{\varepsilon}{\varepsilon_{pc}} \exp \left(1 - \frac{\varepsilon}{\varepsilon_{pc}} \right) \right]^{c} \tag{3}$$

Table 3 provides an example of calculated stress values for ė = 10 s^{-1}. Similar results were obtained with the remaining strain rates values.

Table 3. Calculated stress values at the strain rate of 10 s^{-1}

$\dot{e}$ [s^{-1}]	10		
T [K]	1173	1273	1373
ε	σ_c [MPa]		
0,05	229	179	138
0,1	256	200	153
0,2	280	215	163
0,3	289	219	164
0,4	291	218	161
0,5	290	214	157
0,6	286	209	151
0,7	280	202	144

Graphical plots of the results are shown in the following figures. They include the stress-strain vs. temperature curves in Fig. 2. They also cover the stress-strain vs. strain rate curve in Fig. 3.

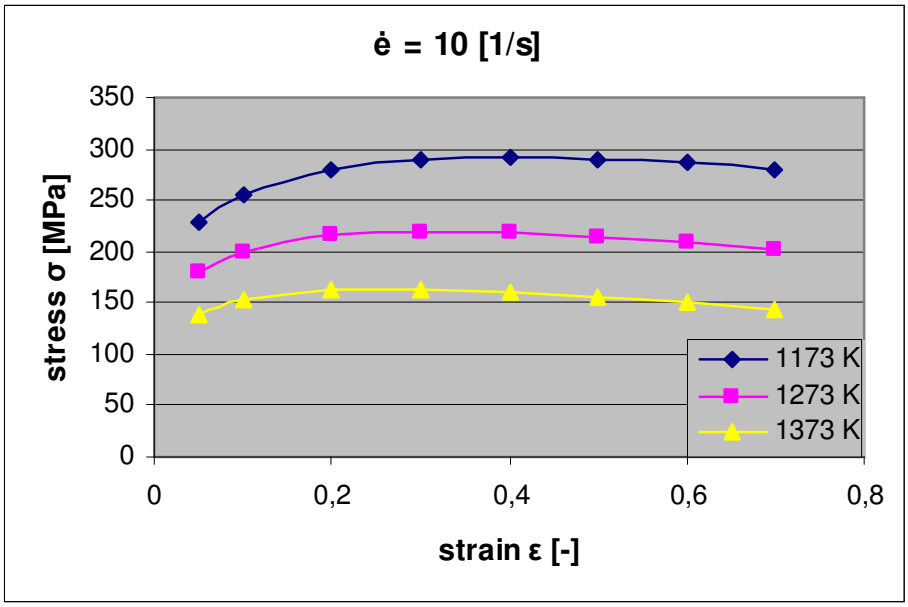

Fig. 2. Stress-strain relationship at the strain rate of 10 s^{-1}

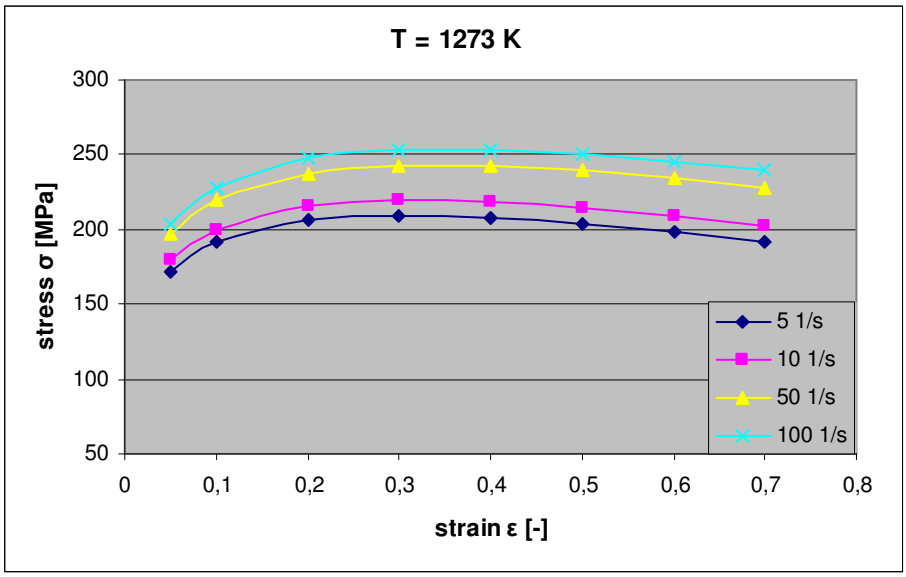

Fig. 3. Stress-strain relationship at the temperature of 1273 K

The experiments include interrupted tests as well. Like continuous tests, they yielded a large number of values which had to be reduced in a similar fashion. Figure 4 shows the stress-strain curves as an example of an actual experiment. The chart contains 3 plots of interrupted tests (p13, p14, p15) and one continuous loading curve (p5) recorded under identical conditions except for different strain rates: 1 s^{-1} and 5 s^{-1}.

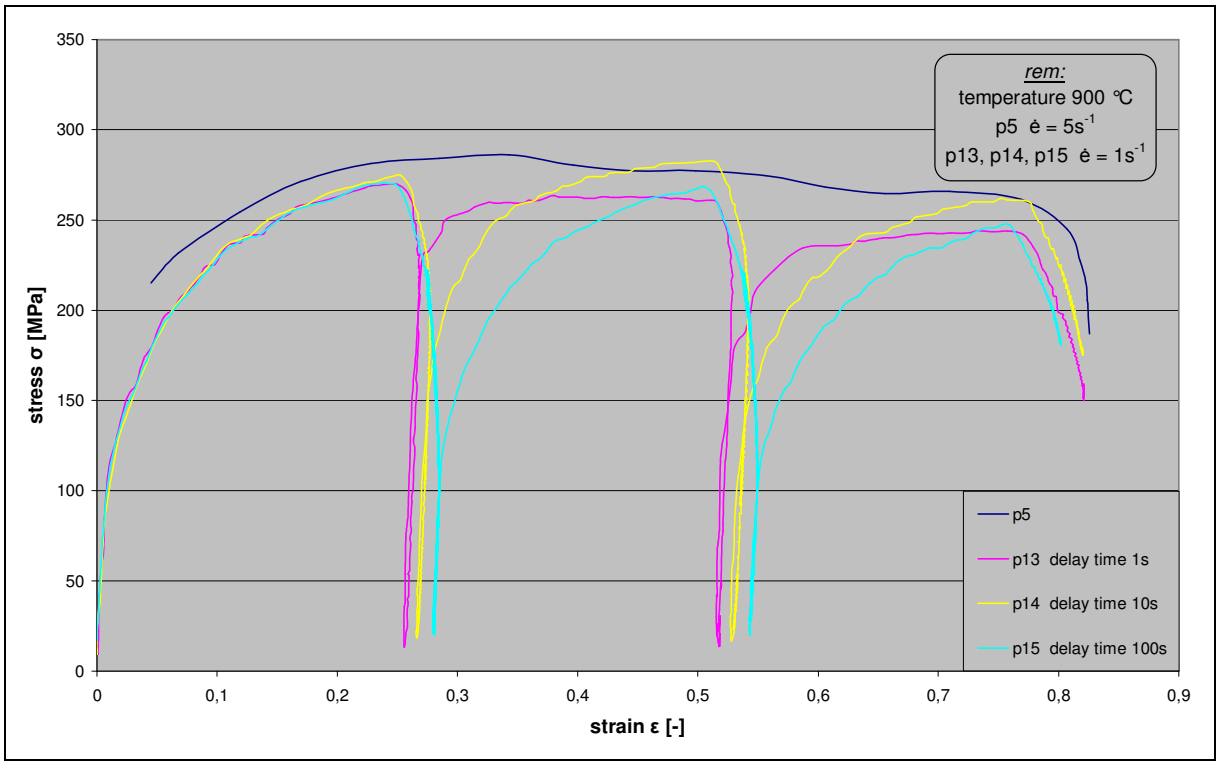

Fig. 4. Comparison of stress-strain relationships for specimens p5, p13, p14, p15

Interrupted tests were performed at all temperatures. Strain magnitudes used were 0,25 and 0,3, respectively. Delays between individual deformation steps were 1, 10 and 100 seconds.

Fig. 4 also includes an envelope curve of the continuous test, owing to which it is possible to estimate the strains at the onset of dynamic recrystallization. Continuous deformation curves are peculiar in showing transition to stationary flow of metal and no inflexion points.

The degree of softening X was calculated for the interrupted test conditions using the following equation.

$$X = \frac{\sigma_m - \sigma_2}{\sigma_m - \sigma_1} \tag{4}$$

Calculated values of X for specimens p10, p11 and p12 are shown in Table 4. The graphical plot of the softening degree vs. time between deformation steps (1, 10 and 100 seconds) is shown in Fig. 5.

Table 4. Values of X for specimens p10, p11 and p12

$\dot{e}$ [1/s]	temperature [°C]	specimen	σ_1 [MPa]	σ_2 [MPa]	σ_m [MPa]	X	delay time [s]
10	1100	P10	123,33	124,83	180,48	0,97	1
		P11	118,82	120,00	188,00	0,98	10
		P12	127,84	138,37	189,50	0,83	100

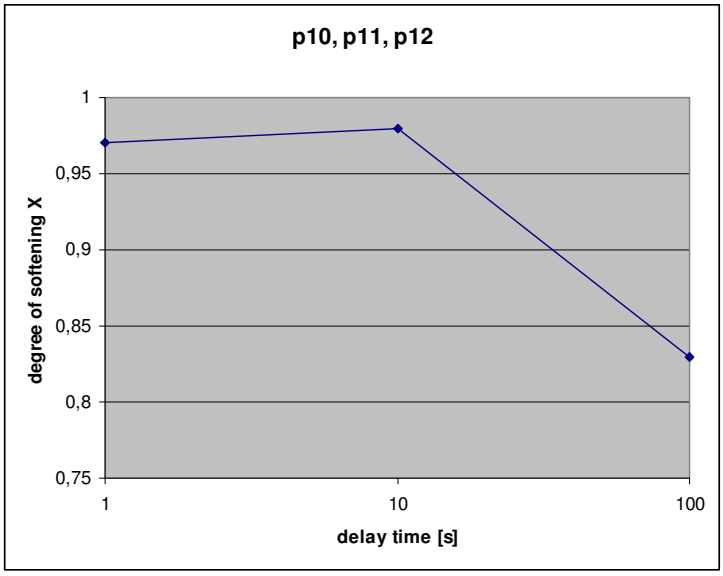

Fig. 5. Degree of softening X in specimens p10, p11 and p12 in relation to delay times

Calculated values of X for specimens p16, p17 and p18 are shown in Table 5. The graphical plot of the softening degree vs. time between deformation steps (1, 10 and 100 seconds) is shown in Fig. 6.

Table 5. Values of X for specimens p16, p17 and p18

ė [1/s]	temperature [°C]	specimen	σ_1 [MPa]	σ_2 [MPa]	σ_m [MPa]	X	delay time [s]
10	900	P16	149,97	215,74	278,89	0,49	1
		P17	181,54	268,36	313,16	0,34	10
		P18	171,02	231,53	305,26	0,55	100

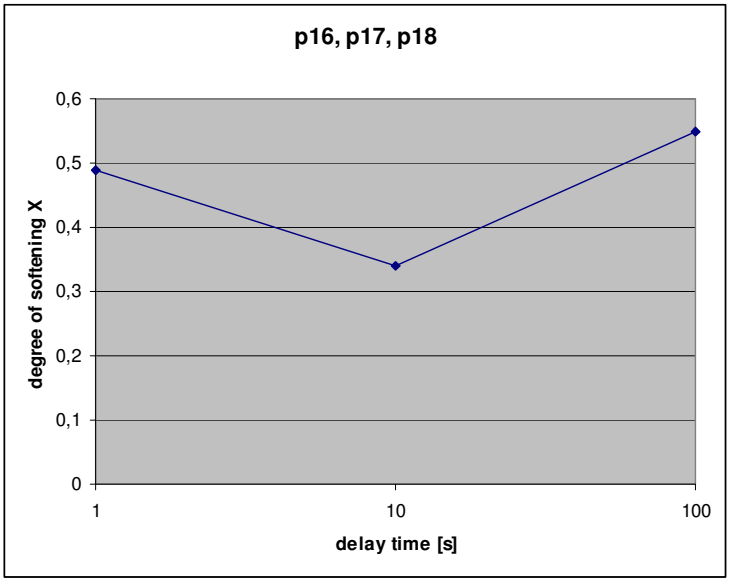

Fig. 6. Degree of softening X in specimens p16, p17 and p18 in relation to delay times

3. EVALUATION OF RESULTS

3.1 Evaluation of continuous loading tests

Initially, at low strain, the curves have normal shape. At higher temperature, the curve follows lower strain values, i.e. stress decreases with increasing temperature. The onset of hardening is very intensive, taking place immediately upon transition of the material to plastic state. It is due to an increase in dislocation density resulting from the deformation process. With further increase in strain, the strain rate decreases owing to concurrent dynamic recovery. At certain strain level, dynamic recrystallization starts. This dynamic process is related to the peaks observed in all three curves. At high temperature: 1100°C, the estimated peak strain is about 0,25, while at 900°C, a value around 0,3 can be expected. Even at 900°C the peak is still high and the state of dynamic recrystallization can be determined [2].

Fig. 3 shows that the effect of strain rate is not particularly strong. The deformation resistance naturally increases with increasing strain rate.

3.2 Evaluation of interrupted tests

For the purpose of graphical comparison, the chart in Fig. 4 contains 3 plots of interrupted tests (p13, p14, p15) and one continuous loading curve (p5) recorded under identical conditions except for different strain rates: 1 s^{-1} and 5 s^{-1}. There is a peak on the continuous test curve at the strain of about 0,3. At the same numerical value of strain rate, the stress approaches an identical peak value during the first stage of the interrupted test.

Assuming that the first deformation stage takes place in the peak region (the peak strain and stress values determined by means of plastometric tests correspond to an already active dynamic recrystallization, which began to take place in the structure even before the peak stress and strain were achieved), it appears that after the delays the dynamically recrystallized grains begin to grow and metadynamic recrystallization begins to take effect. It seems that the continuous deformation curve forms an envelope curve for the interrupted deformation plots. Similar results were achieved with the remaining curves [2].

Interrupted tests of the current steel grade at the testing temperature have demonstrated a rapid start of recovery. In a high-manganese TWIP steel, this can be attributed to its typical austenitic microstructure. The subsequent start of dynamic recrystallization makes it impossible to perform the classical calculation of degree of recovery X, which is normally used for description of static recrystallization. The value for dynamically recovered microstructure at 1100 °C approaches 1 and shows only slight decrease with increasing delay between deformation steps. This decrease might be attributed to the capabilities and potential of experimental evaluation. Results shown in table 4 fall within the range of error in measurement and the reading error. At the lowest temperature of 900 °C, where the peak occurs at values higher than 0,4 – as evidenced by the previous continuous stress-strain curves – the degree of recovery of microstructure is 0,5 or less. Gradual increase with the value of X and increasing length of delays between deformation steps can be expected.

4. CONCLUSION

Specimens were processed in the Gleeble thermal-mechanical simulator in 18 cycles as indicated in the diagrams in Fig. 1 and 2. The processing cycles comprised different temperatures, amounts of deformation, strain rates and, for some specimens, different delays between deformation steps and cooling modes. Continuous tests were performed at 1100, 1000 and 900 °C, with the strain of 0,8 strain rate of 5 s^{-1}. It was found that the shapes of curves indicate the occurrence of dynamic recovery and, at certain strain level, even the dynamic recrystallization, which is evidenced by the stress peaks on all curves.

Parameters of interrupted tests included delays of 1, 10 and 100 s, strain rates of 1 and 10 s^{-1} and strain magnitudes in individual deformation steps of 0,25 and 0,3, respectively, at 900 and 1000 °C. An analysis of the results shows that dynamically recrystallized grains begin to grow after the delay and the process is characterized by metadynamic recrystallization. It appears that the continuous deformation curve forms an envelope curve for the interrupted deformation plots.

REFERENCES

[1] KLIBER, J., KURSA, T., SCHINDLER, I.: The Influence of Hot Rolling on Mechanical Properties of High-Mn TWIP steel. In 3rd Int. Conf. Thermomechanical Processing of Services. Brno: Tribun EU Brno, 2008, s. 125-130. ISBN 978-80-7399-420-3.

[2] KURSA, T.: *Diplomová práce*, FMMI, VŠB-TU Ostrava, 2008.
[3] KLIBER, J.: Simulation of forming processes by plastometric tests. Sborník vědeckých prací Vysoké školy báňské – Technické univerzity Ostrava, číslo 1, 1997, řada hutnická, článek č. 1169.
[4] KLIBER, J. - SCHINDLER, I.: Deformation resistence during metal forming. In. Proc. 4th Europen Conference Euromat 95, Padova, Italy, September 1995, Symp. F. p.-94.
[5] KLIBER, J.: New approaches in describing stress-strain curves. In: Procedings Inter. Conf. FORMABILITY 94, October 1994, Tanger Steel, Ostrava, pp. 77-83.
[6] SCHINDLER, I. – KLIBER, J.: Deformation Resistance and Static Softening Behavior of Type Mo-Nb-V Microalloyed Steels Determined by Plastometric Experiments. In: ICSMA 9. Int. Conference, Haifa, Israel, s. 1151-1158.
[7] KLIBER, J – SCHINDLER, I. – BOŘUTA, J.: Deformation resistence of materials (Activation Energy) – Part I. In: Int. Conf. CAD in metal forming. Wisla, Poland, January 1995, pp. 211-213.
[8] KLIBER, J. – SCHINDLER, I.: Stress-strain curves computer modelling of deformed steel at elevated temperatures. In. Proc. ICSMA 9th Inter. Conference, Haifa, Israel, p. 647-654.
[9] RYAN, N.D. – QUEEN, MC., H.J.: Flow stress, dynamic restiration, strain hardening and ductility in hot working of 316 steel. Journal of Mechanical Working Technology, 21, ,p. 177-199.
[10] CINGARA, A. – QUEEN, MC., H.J.: In Inter. Symposium on Processes, Pensylvania, 1987.